


Transient growth and dissipative exceptional points

K. G. Makris

*ITCP-Physics Department, University of Crete, 71003 Heraklion, Greece
and Institute of Electronic Structure and Laser, FORTH, 71110 Heraklion, Greece* (Received 27 August 2021; accepted 19 September 2021; published 30 November 2021)

In the context of non-Hermitian photonics, we study the physics of transient growth in coupled waveguide systems that exhibit higher-order exceptional points. We demonstrate the counterintuitive effect of transient growth despite the decaying spectrum, which is a direct consequence of the underlying modal nonorthogonality. Eigenvalue analysis fails to capture the power dynamics and thus we have to rely on methods of nonmodal stability theory, namely singular value decomposition and pseudospectra. The relation between the order of the exceptional point and transient growth is also examined. Our work provides a general methodology that can be applied to any non-Hermitian system that contains complex elements with more loss than gain, and exploits the boundaries of transient amplification in dissipative environments.

DOI: [10.1103/PhysRevE.104.054218](https://doi.org/10.1103/PhysRevE.104.054218)**I. INTRODUCTION**

Non-normality is a mathematical property of crucial importance and relevance in various fields of physics. Generally speaking an operator or a matrix \hat{M} is non-normal [1], i.e., it does not commute with its adjoint $[\hat{M}, \hat{M}^\dagger] \neq 0$. When the underlying Hamiltonian is non-normal then the study of the spectral problem, as well as the evolution dynamics, is a highly nontrivial issue. Of particular interest is the counterintuitive effect of transient growth despite the underlying dissipative spectrum. In fact, the physics of transient growth has attracted a lot of attention and plays central role in the context of turbulence in fluid mechanics [2–4], non-normal network theory [5–7], nonmodal stability methods [8,9], and excess noise in laser physics [10–16].

In a seemingly unrelated direction, the engineering of the complex refractive index to create new composite systems with novel functionalities is one of the forefronts of modern photonics. For more than 30 years several novel photonic lattice structures have been investigated for the efficient control and manipulation of light [17]. One fundamental problem though is the existence of optical losses due to the inherent absorption of the materials. As a result, engineering of the imaginary part of the index of refraction is at the technological frontier of integrated photonics and of great importance for various fields, especially that of active nanoplasmonics, and metamaterials. In most systems optical loss has been always considered an obstacle. However, based on the recently introduced concept of parity-time (\mathcal{PT}) symmetry [18–20] in the context of optical physics [21–26], such synthetic structures can utilize loss as an advantage and have been proven to be important for various nanophotonics applications. As the paradigm of parity-time symmetric optics [21–26], indicates, the resolution of this problem is the judicious combination of gain and loss as an extra degree of freedom for creating a new generation of loss-free optical metastructures and systems with novel functionalities, both in micro- and nanoscale [27–33].

Such complex structures have been experimentally realized with optical waveguides, fiber networks, as well as with microcavity lasers and represent a class of optical systems where the deliberate introduction of loss and its spatial distribution along with gain can achieve new functionalities with potential applications, as new type of metamaterials [34,35], active plasmonic devices [36–38], and as optical isolators, and switches [39–47]. Furthermore, exceptional points are unique spectral singularities characteristic of non-Hermitian Hamiltonians. At these singular points in the parameter space, both N eigenvalues and the corresponding N eigenstates coalesce forming a higher-order exceptional point (HEP) of N th order (EPN) [48–59]. This new area of optical physics, namely non-Hermitian photonics [60–67] is the physical context of our work, even though the presented methodology can be generally applied in any non-normal dissipative system.

Recent experiments [25,26], however, have demonstrated that in most photonic applications it is challenging to fabricate optical structures in which optical loss and gain are perfectly balanced. Thus the most general situation of non-normal dissipative potentials, where the overall loss generally dominates over the optical gain, needs to be systematically studied. At this point is where the synergy between non-Hermitian photonics and non-normal physics is crucial for the further understanding of optical transient growth and dissipation engineering. This direction is largely unexplored in the non-normal optics literature [11–14,68–72] and may have potential applications for transient power amplification and active plasmonic systems.

In this paper we investigate the physics of transient growth of optical power in non-Hermitian coupled waveguide systems that are spectrally lossy, and exhibit higher-order exceptional points. As a result, these systems are dissipative in the sense that all eigenvalues correspond to eigenstates that decay with propagation distance, and thus lie on the left half of the complex plane. In other words, such systems exhibit zero modal gain despite the fact that the material gain is

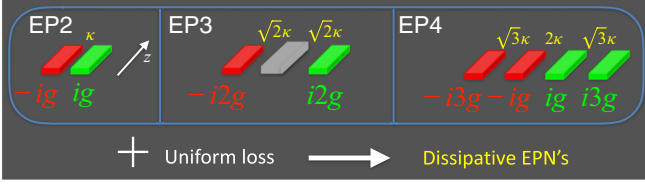


FIG. 1. Schematic depiction of non-normal photonic waveguide structures that exhibit dissipative higher-order exceptional points. In all figures the green, gray red regions represent the lossy, neutral dielectric, and gainy regions, respectively. The propagation axis is denoted with z and a white arrow, and the coupling coefficients are denoted with yellow. The three \mathcal{PT} -symmetric waveguides structures that exhibit EP2, EP3, EP4, are shown in the corresponding boxes. After a global gauge transformation, these lattices become dissipative.

nonzero. Based on our notion of eigenvalues one would expect that the total optical power decays with increasing propagation distance. But that is not true since the eigenstates are nonorthogonal and thus transient amplification is physically allowed. In order to understand the underlying mechanism, we have to rely on methods on non-normal physics, such as singular value decomposition, pseudospectra, and matrix resolvents that go beyond the eigenvalue analysis of the associated non-normal operator [1–4]. More specifically, these coupled structures exhibit transient power growth, the magnitude of which is related to the singular values of the non-normal propagator whereas the optimal initial condition to its right singular eigenstates. The nontrivial wave dynamics in such non-Hermitian optical systems can be estimated in terms of the pseudospectra (Kreiss matrix theorem) of the evolution non-normal operator. The interplay between the extreme sensitivity around EPN's and transient growth is also discussed. The systematic examination of these highly nontrivial and basic questions regarding the transient amplification of decaying waves around dissipative higher-order exceptional points is the main focus of this paper.

II. DISSIPATIVE PHOTONIC STRUCTURES

Even though our methodology is quite general and can be applied in any non-normal dynamical system, we are interested on the physically relevant structures of coupled waveguide channels that can be experimentally implemented [59]. Let us consider the propagation of optical waves in spatially complex photonic structures [17] with a preferred axis for propagation (z) characterized by a complex index of refraction modulation profile, such as the structures that are graphically depicted in Fig. 1. Under the paraxial approximation, the dynamics of the slowing-varying field amplitude can be captured by the paraxial equation of diffraction (Schrödinger-like equation), which can be further discretized in the framework of coupled mode theory (tight binding approximation). Thus the normalized paraxial coupled mode equations that govern the wave dynamics are [17]:

$$i \frac{\partial \psi_n}{\partial z} + \kappa(\psi_{n+1} + \psi_{n-1}) + \epsilon_n \psi_n = 0, \quad (1)$$

where n is the index number ($n = 1, \dots, N$), z is the propagation distance, ψ_n and ϵ_n are the complex peak amplitude of the envelope of the electric field and the field propagation constant of the n th channel (which here plays the role of the on-site energy or potential strength) and κ is the coupling constant between nearest neighbors. The non-Hermiticity of our problem stems from the fact that the potential is complex, meaning that: $\epsilon_n = \text{Re}(\epsilon_n) + i\text{Im}(\epsilon_n)$ where positive values of $\text{Im}(\epsilon_n) > 0$ correspond to physical material loss (wave dissipation), whereas negative values correspond to physical material gain (wave amplification). We note here that the material gain or loss of the system is directly related to the sign of the imaginary part of the potential strength.

We can express the above system of N -coupled ordinary differential equations in a compact dynamical system form as:

$$\frac{\partial |\psi\rangle}{\partial z} = \hat{M} |\psi\rangle, \quad (2)$$

where \hat{M} is the evolution matrix of the system, and $|\psi\rangle = [\psi_1, \psi_2, \dots, \psi_N]^T$ is the amplitude vector. Here \hat{M} a non-Hermitian matrix of dimensions $N \times N$, which is generally non-normal [1], since the ϵ_n is complex.

For the spectral properties of our model, we will consider modal solutions of the form: $|\psi\rangle = |u_n\rangle e^{\lambda_n z}$, where λ_n is a generally complex eigenvalue and the $|u_n\rangle$ the corresponding right eigenstate of the right non-Hermitian eigenvalue problem is $\hat{M}|u_n\rangle = \lambda_n|u_n\rangle$. In particular, $\lambda_n = \gamma_n + i\beta_n$ thus is in generally complex, where positive values of $\gamma_n > 0$ correspond to growing mode (right half complex plane), whereas negative values $\gamma_n < 0$ correspond to a decayed mode (left half of the complex plane). It is important to notice here that the modal gain or loss of each eigenstate is directly related to the imaginary part of the corresponding eigenvalue. More specifically, if $\gamma_n > 0$ ($\gamma_n < 0$), then the n th eigenstate has modal gain (loss).

Now by applying a global gauge transformation [25] on the corresponding \mathcal{PT} -symmetric coupled structures that exhibit EPN's [71], we can construct systems that exhibit dissipative EPN's. By the term “dissipative,” we mean that all spectrum resides on the left half of the complex plane ($\gamma_n < 0, \forall n$). This physically means that we add a uniform loss l to all waveguides and as a result we get the following three evolution matrices:

$$\hat{M}_2 = i \begin{bmatrix} -ig + il & \kappa \\ \kappa & ig + il \end{bmatrix}, \quad (3)$$

$$\hat{M}_3 = i \begin{bmatrix} -i2g + il & \sqrt{2}\kappa & 0 \\ \sqrt{2}\kappa & il & \sqrt{2}\kappa \\ 0 & \sqrt{2}\kappa & i2g + il \end{bmatrix}, \quad (4)$$

$$\hat{M}_4 = i \begin{bmatrix} -i3g + il & \sqrt{3}\kappa & 0 & 0 \\ \sqrt{3}\kappa & -ig + il & 2\kappa & 0 \\ 0 & 2\kappa & ig + il & \sqrt{3}\kappa \\ 0 & 0 & \sqrt{3}\kappa & i3g + il \end{bmatrix}, \quad (5)$$

which exhibit higher-order exceptional points of order two (EP2), three (EP3), and four (EP4), respectively. Here g is the gain-loss amplitude of the system and l denotes the overall loss. Unless is stated otherwise we assume $\kappa = 1$ for all the subsequent results. For the case of zero overall loss,

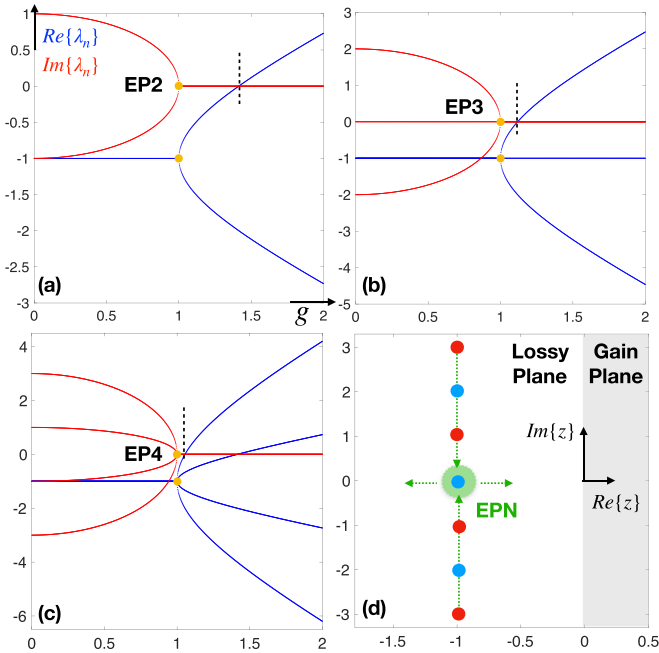


FIG. 2. (a), (b), (c) Eigenvalue spectrum for $l = 1$ plotted as a function of g for the three matrices $\hat{M}_2, \hat{M}_3, \hat{M}_4$, respectively. More specifically, the real (imaginary) part of the complex eigenvalue bifurcation curves are presented with blue (red) color solid lines, respectively. In all three figures the x axis is g , and the yellow dots show the value of g for which we have a HEP in every case. The vertical dashed black line segments show the crossing to the right half complex plane. (d) Eigenvalue trajectories of the three matrices in the complex plane as g varies. The dashed-green arrows indicate graphically the path that the complex eigenvalues follow in the complex plane. The light gray shaded area denotes the right half of the complex plane that corresponds to amplifying eigenstates, whereas the left half plane corresponds to decayed eigenmodes.

namely $l = 0$, all the corresponding three Hamiltonians are \mathcal{PT} -symmetric and exhibit HEP, power oscillations, and amplification [71]. What we are interested to investigate in this work is what happens to the power dynamics under a global gauge transformation.

Let us first examine the eigenvalue spectrum of the problem as a function of gain-loss amplitude g for fixed overall loss $l = 1$. Our results are shown in Fig. 2. In Fig. 2(d) a graphical depiction of the eigenvalue trajectories in the complex plane is shown. In all three cases, the eigenvalues coalesce at the same point of the complex plane [the $(-1, 0)$ point] for $g_{HEP} = 1$, and then bifurcate into the real axis, as the green arrows indicate. More specifically, the complex eigenvalue curves versus the gain-loss parameter g are presented in Fig. 2, for both the real (blue lines) and imaginary parts (red lines) of the corresponding eigenvalues. In particular, we can clearly see in Figs. 2(a)–2(c) the existence of the HEPs (yellow dots) where all eigenvalues and eigenvectors coalesce. For some critical value of g_c one of the eigenvalues will cross the right half complex plane (gain plane) and thus we expect asymptotically an exponential amplification. For $g > g_c$ the system displays a transition to a globally amplifying behavior, i.e., in the asymptotic $z \rightarrow \infty$ limit, the power increases exponentially. This is found to be consistent with an eigenvalue of the system

crossing over to the gain plane. The vertical dashed black line segments denote the values ($g_c \approx 1.4, 1.11, 1.05$) of g for which such a transition occurs. The question is what happens below these values. Based on our notion of eigenvalues, and since they all have negative real part (which physically means that modal gain is zero and thus all eigenstates decay with z), we expect that the total optical power will decay with increasing propagation distance. As we will see in the next paragraphs, this expectation is true only asymptotically for large values of z . Because of the underlying nonorthogonality, transient power growth is possible, for particular optimal initial conditions.

Such questions are directly related to the growing field of active plasmonics, and in particular to the optical switching in coupled \mathcal{PT} -symmetric plasmonic systems [36]. Unlike these previous studies, our work applies the most general approach to understand and quantify the power growth in any dissipative system that has an amount of gain, but still is overall lossy. In view of the above, we believe that the answers to our questions will have important implications to the efficient design of active plasmonic devices.

III. AMPLIFICATION, DISSIPATION, AND TRANSIENT GROWTH

A unique characteristic of any non-Hermitian system with spatially inhomogeneous distribution of gain and loss is that, in principle, amplification and/or dissipation is possible on the same device because of the nonconservation of optical power. This effect is called power oscillations in the context of \mathcal{PT} -symmetric optics [22,24]. Since gain and loss compose the photonic structure, the eigenmodes are nonorthogonal and as a consequence we have bounded oscillations of the power (integrated intensity) with respect to the propagation distance z . More specifically, below an exceptional point, the power oscillates with propagation distance z (unbroken symmetry regime), whereas above the exceptional point (broken symmetry regime) it grows exponentially.

The situation is more complex in the case of dissipative exceptional points. In particular, instead of the two regimes, that of power oscillations and exponential amplification (for example in a \mathcal{PT} -symmetric lattice), here we identify three different regimes depending on the value of g , namely: dissipation, amplification, and transient growth. The power dynamics and its dependence with z is of particular physical interest and is the center of our work. One possible way to characterize fully any non-Hermitian system is by using methods of nonmodal stability theory of fluid mechanics [73,74], and in particular, pseudospectra and singular value decomposition. This approach can provide us the optimal initial conditions for the maximum amplification ratio for a specific value of the propagation distance.

Before we establish the mathematical framework to analyze such complex behavior, it is crucial to define the main (measurable observable) quantity of interest in our study, which is the optical power P , that is defined as:

$$P(z) \equiv \sum_{n=1}^N |\psi_n(z)|^2 = \|\psi\|^2, \quad (6)$$

where $\|\psi\|^2 = \langle \psi | \psi \rangle$ is the usual Euclidean norm of the ket $|\psi\rangle$. It is easy to show that in the Hermitian limit the power is a conserved quantity of the lattice, because the eigenmodes are orthogonal. In our case, due to the complex values of the potential strength per site, the eigenstates are nonorthogonal and as a direct outcome the power is not a conserved quantity anymore but a function of the propagation distance z . We can gain some physical insight regarding the power dynamics by directly calculate the derivative of the power with respect to the propagation distance. We can derive the following general expression:

$$\frac{dP}{dz} = -2 \sum_{n=1}^N \text{Im}(\epsilon_n) |\psi_n(z)|^2. \quad (7)$$

If all elements of our lattice are lossy, meaning that $\text{Im}(\epsilon_n) > 0, \forall n$ then $\frac{dP}{dz} < 0, \forall z$ and as a result we have decay of the wave for any initial condition. In this case we are in the dissipation regime [72], meaning that we have nonzero material loss and modal loss, and also zero material gain-modal gain. In other words, the first element (1,1) of the three evolution matrices corresponds to the maximum material gain and thus its sign marks the transition from the dissipation regime to the transient growth. This crossover happens for $g = l = 1$, $g = l/2 = 0.5$, and $g = l/3 = 0.33$, respectively.

On the other hand, if one of the eigenvalues λ_n is gainy then we expect amplification. This marks the amplification regime, where we have nonzero modal gain, $\gamma_n > 0$, for some n . Now the most interesting regime that is the focus of our work, is the case where all eigenvalues correspond to loss but there is still material gain. Then we physically expect the possibility of transient growth of the wave for particular initial conditions before the asymptotic decay. In this transient growth regime we have nonzero material loss-modal loss, and zero modal gain $\gamma_n < 0, \forall n$ but nonzero material gain, $\text{Im}(\epsilon_n) < 0$ for some n . More specifically, the change of sign of the first element of all three \hat{M} matrices above some value of g indicates the possibility of transient growth.

In order to describe quantitatively the power dynamics we define the power amplification ratio G at a particular propagation distance z , which is defined as:

$$G(z) = G(z, g, l, \psi_0) \equiv \frac{P(z)}{P(0)} = \frac{\|\psi(z)\|^2}{\|\psi(0)\|^2}, \quad (8)$$

where $|\psi_0\rangle \equiv |\psi(z=0)\rangle$ are given the initial conditions at $z=0$. Obviously, the $G(z)$ depends strongly on the initial conditions, on the gain-loss g and loss l parameter. Thus physically relevant quantities are the maximum power amplification ratio (output over input power) G_{\max} , its maximum value G_{\max}^{\max} with respect to all z 's and the maximum value of the last one with respect to all g 's. These quantities are defined as follows:

$$G_{\max}(z, g, l) \equiv \max_{\|\psi(0)\|} G(z) \quad (9)$$

$$G_{\max}^{\max}(g, l) \equiv \max_z G_{\max}(z) \quad (10)$$

$$mG_{\max}^{\max}(l) \equiv \max_g G_{\max}^{\max}. \quad (11)$$

Notice that the for a given value of z there is a particular value of G_{\max} that is achieved by a particular initial condition. The maximum is over all possible normalized initial condi-

tions ($\|\psi(0)\| = 1$). Therefore for different z 's the maximal growth is due to different set of initial conditions. Thus all the three quantities are global properties that characterize the system over all possible initial conditions. The physical question that we are interested to answer is: how much is G_{\max} in coupled optical waveguides that exhibit higher-order exceptional points and under what conditions their enhanced sensitivity contributes to transient growth. Our ultimate goal is to provide a computational framework of quantifying the transient growth in situations that the material gain is much less than the material loss, but still transient amplification is possible. The approach we are going to follow has two related paths. Initially, we are going to solve our optimization problem [which is defined by the above Eq. (9)] exactly by numerically evaluating the norm of the exponential matrix and its singular values. Secondly, we will estimate such maximal power growth by applying the novel geometrical concept of pseudospectrum.

IV. TRANSIENT GROWTH: EXPONENTIAL MATRIX APPROACH

Since our problem is linear and the \hat{M} matrix is z independent, the dynamical equation of motion can be directly solved, in terms of the exponential matrix of the problem:

$$|\psi(z)\rangle = e^{z\hat{M}} |\psi_0\rangle. \quad (12)$$

At this point is useful for the subsequent analysis to define the following matrix \hat{G} for a given value of the propagation distance z as:

$$\hat{G}(z) \equiv e^{z\hat{M}}. \quad (13)$$

Based on the fact that the norm of a matrix is generally defined as $\|\hat{G}\| \equiv \max_{\|\psi(0)\|} \|\hat{G}\psi\|/\|\psi\|$, we can determine the maximal amplification ratio G_{\max} from the following relation:

$$G_{\max}(z) = \max_{\|\psi(0)\| \neq 0} \frac{\|\psi(z)\|^2}{\|\psi(0)\|^2} = \|e^{z\hat{M}}\|^2 = \|\hat{G}(z)\|^2, \quad (14)$$

where the right-hand side is the square of the matrix norm of the propagator of the system $\hat{G} = e^{z\hat{M}}$. At this point we have to note the conceptual difference of the growth ratios described by Eqs. (8) and (14). In the first case G is the ratio of the output over input power for a specific initial condition. On the other hand, Eq. (14) describes the maximum amplification ratio for all possible initial conditions at $z=0$. Our results regarding the maximal growth $G_{\max}(z)$ are shown in Fig. 3. More specifically, in Figs. 3(a)–3(c) we illustrate $G_{\max}(z)$ versus z for the three $\hat{M}_2, \hat{M}_3, \hat{M}_4$ matrices, respectively, for 15 different values of the gain-loss parameter g . The blue solid lines correspond to the transient growth regime for different values of g , the green dot-dashed lines the dissipation regime and the red dashed lines to the amplification regime. Based on the quantities G_{\max} and G_{\max}^{\max} we can distinguish the three different regimes, namely: dissipation when $G_{\max}^{\max} = 1$, transient growth when $G_{\max}^{\max} > 1$, and amplification when $G_{\max}^{\max} = \infty$. In the regimes of dissipation and transient growth is also true that $\lim_{z \rightarrow \infty} G_{\max}(z) = 0$. But still the optimal initial conditions that lead to the maximal transient growth are so far unknown and we will use a different approach to determine them. The relation between the singular spectrum of the propagator and

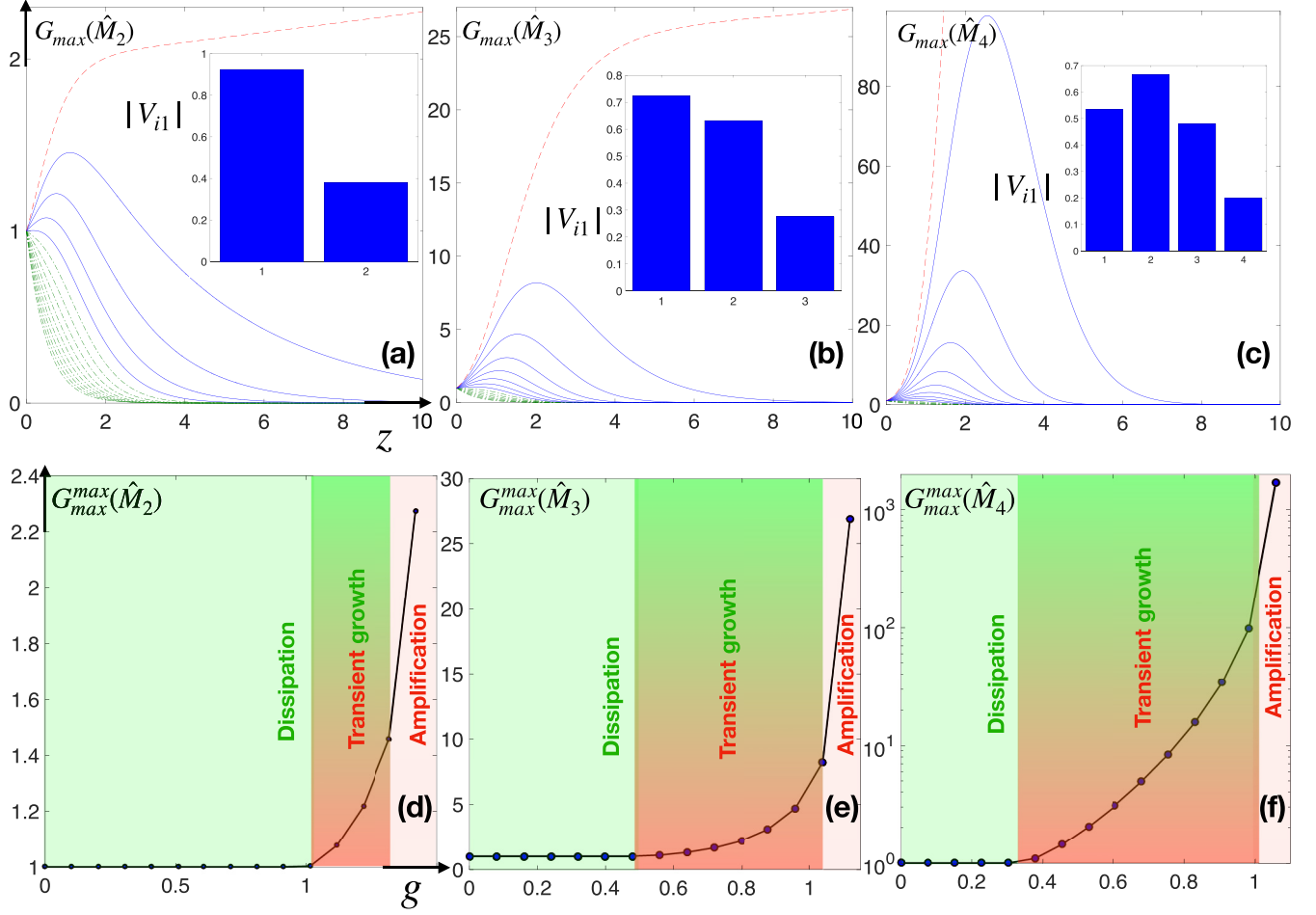


FIG. 3. (a), (b), (c) $G_{\max}(z)$ versus z (same axes) for the three matrices, respectively, for 15 different values of g from 0 up to 1.419, 1.119, 1.058, respectively. In all three figures, the red dashed lines correspond to amplification, the blue solid lines to transient amplification, and the green dot-dashed lines the dissipation. The insets show the amplitude of the first column elements of V_{i1} -matrix of the optimal initial conditions (right singular vectors of the propagator, given by Eq. (20) when $n_0 = 1$, due to the sorting of the singular values) that lead close to the maximum value of the G_{\max}^{\max} for all g 's. (d), (e), (f) Plot of G_{\max}^{\max} for $l = 1$ versus g , for the three \hat{M} matrices (same axes). In (e) logarithmic scale was used for the depiction of the result. The schematic shaded colored areas correspond to a different regime, namely green: dissipation; green/red: transient growth; and red: amplification. Their exact boundaries in (d), (e), (f) are determined by the values: 1, 0.5, 0.33 (dissipation-growth boundary) and 1.4134, 1.1171, 1.0531 (growth-amplification boundary), respectively.

these optimal conditions is going to be examined in the next section.

V. TRANSIENT GROWTH: SINGULAR VALUE DECOMPOSITION APPROACH

So far we have not analyzed the optimal initial conditions that lead to the maximum transient growth at a given value of z . We show below that the initial conditions for maximum amplification are complicated and most remarkably are not localized only at the gain regions, as one may intuitively expect. Here we follow a rigorous and numerically exact method based on the singular value decomposition (SVD) of the non-Hermitian propagator $\hat{G}(z)$ in order to determine these optimal initial conditions for a given structure. This means that we can decompose the matrix $\hat{G}(z)$ as $\hat{G}(z) = \hat{U} \hat{\Sigma} \hat{V}^\dagger$. The columns of \hat{U} are called left singular vectors, the columns of \hat{V} are called right singular vectors, and the diagonal elements of $\hat{\Sigma}$ are called singular values $\{s_n\}$. The two related eigenvalue

problems are

$$\hat{G}|v_n\rangle = s_n|v_n\rangle, \quad \hat{G}^\dagger|v_n\rangle = s_n|v_n\rangle, \quad (15)$$

where $\{|v_n\rangle\}$, $\{|v_n\rangle\}$ are the orthonormal sets of the right and left singular eigenstates, respectively. We note that the singular values s_n are real and non-negative even for a non-Hermitian matrix. Also we can directly show that the squares s_n^2 are the eigenvalues of the Hermitian matrix $\hat{G}^\dagger \hat{G}$, since it is true that:

$$\hat{G}^\dagger \hat{G}|v_n\rangle = s_n \hat{G}^\dagger |v_n\rangle = s_n^2 |v_n\rangle. \quad (16)$$

Intuitively speaking, one would expect that if the input waveform is coupled to the gain regions only, it probably will lead to the maximum power growth. This is, however, not true as we show below.

Since it is by definition true that $\|\hat{G}\|^2 = \max_{\|\psi_0\| \neq 0} \frac{\|\hat{G}\psi_0\|^2}{\|\psi_0\|^2}$, we have the following:

$$\|\hat{G}\|^2 = \max_{\|\psi_0\|} \frac{\langle \hat{G}\psi_0 | \hat{G}\psi_0 \rangle}{\|\psi_0\|^2} = \max_{\|\psi_0\|} \frac{\langle \psi_0 | \hat{G}^\dagger \hat{G} \psi_0 \rangle}{\|\psi_0\|^2}. \quad (17)$$

It is easy to see that if $|\psi_0\rangle = |v_n\rangle$ then $\|\hat{G}\|^2 = \max_n \{s_n^2\}$, which practically means that the eigenvector corresponding to the largest eigenvalue of the Hermitian operator $\hat{G}^\dagger \hat{G}$, which is exactly the right-singular vector of \hat{G} with the largest s_n , maximizes the amplification ratio. In other words, the conclusion can be written as for a particular value of z :

$$n_0 \equiv \{n_0 \in \mathcal{N} : \max_n \{s_n^2\} = s_{n_0}^2\} \quad (18)$$

$$G_{\max}(z) = \|\hat{G}(z)\|^2 = s_{n_0}^2 \quad (19)$$

$$|\psi_0\rangle = |v_{n_0}\rangle. \quad (20)$$

The above conclusion can be rigorously derived by expanding the arbitrary ket to the right singular eigenstates that form an orthonormal basis. In other words, we have:

$$|\psi_0\rangle = \sum_{n=1}^N c_n |v_n\rangle \quad (21)$$

$$\hat{G}^\dagger \hat{G} |\psi_0\rangle = \sum_{n=1}^N s_n^2 c_n |v_n\rangle, \quad (22)$$

where c_n are the corresponding projection coefficients. Based on the orthonormality conditions $\langle v_m | v_n \rangle = \delta_{n,m}$ we have the following for the $\|\psi_0\|^2 = \langle \psi_0 | \psi_0 \rangle$:

$$\langle \psi_0 | \psi_0 \rangle = \sum_{n,m=1}^N c_m^* c_n \langle v_m | v_n \rangle = \sum_{n=1}^N |c_n|^2. \quad (23)$$

Similarly we have for the $\langle \psi_0 | \hat{G}^\dagger \hat{G} \psi_0 \rangle$ the following:

$$\langle \psi_0 | \hat{G}^\dagger \hat{G} \psi_0 \rangle = \sum_{n,m=1}^N s_n^2 c_m^* c_n \langle v_m | v_n \rangle = \sum_{n=1}^N |c_n|^2 s_n^2. \quad (24)$$

By combining the two last relations we get the general expression for the amplification ratio $G(z)$:

$$G(z) = \frac{\sum_{n=1}^N |c_n|^2 s_n^2}{\sum_{n=1}^N |c_n|^2}, \quad (25)$$

which lead us to the following inequality for the maximum power growth:

$$\sum_{n=1}^N |c_n|^2 s_n^2 \leq s_{n_0}^2 \sum_{n=1}^N |c_n|^2 \quad (26)$$

which completes our derivation.

Our results regarding G_{\max}^{\max} are presented in Fig. 3. In particular, in Figs. 3(d)–3(f) we plot G_{\max}^{\max} versus g for $l = 1$, of all three \hat{M} matrices, respectively. The three different regimes dissipation, transient growth, and amplification, are shown by the three different colored shaded areas green, red/green, and red, respectively. The boundaries of these three areas are in agreement with the previous figures. More specifically, for the values of $g = 1, 0.5, 0.33$ we have the transition from

dissipation ($G_{\max}^{\max} = 1$) to transient growth regime ($G_{\max}^{\max} > 1$), for the three matrices, respectively. Notice that these values coincide exactly with the values of g for which the matrix elements $\hat{M}_i(1, 1)$ change sign. Similarly the critical values of g_c for which we have the transition from transient growth to amplification are $g = g_c \approx 1.41, 1.117, 1.053$ for the three matrices, respectively, which are exactly the same as the values of g corresponding to the black dashed vertical lines shown in Figs. 2(a)–2(c). Regarding the optimal initial conditions that lead to the maximum transient growth G_{\max}^{\max} for the particular z that the maximum occurs, we plot in the insets of Figs. 3(a)–3(c) the magnitude of the corresponding right singular eigenstates for the three propagators, respectively. Notice that there is a significant overlap of the initial field with all channels following a nontrivial amplitude and phase (not shown) profile, which is in contrast to our intuition for maximum overlap with the gain regions only.

VI. TRANSIENT GROWTH: PSEUDOSPECTRUM APPROACH

The previous approach based on exponential matrices and singular value decomposition provided a numerically exact solution to our optimization problem of maximization of the transient growth. A complementary approach based on pseudospectra of a non-normal matrix, though, is still useful since it is a semianalytical way to estimate G_{\max}^{\max} and obtain various relevant bounds. The theory of pseudospectra [1] is well established and widely used in various fields of physics, such as in nonmodal stability problems of fluid mechanics related to turbulence [2], nonlinear dynamics [8], and complex networks [6].

In particular, the ε pseudospectrum $\sigma_\varepsilon(\hat{M})$ of a non-Hermitian matrix \hat{M} is a generalization of its spectrum, denoted here with $\sigma(\hat{M})$, that provides valuable information about the transient growth and the sensitivity of the spectrum against perturbations. There are three equivalent definitions of the pseudospectrum that we are going to use here [1]. The first one defines the ε pseudospectrum as the union of all the spectra in the complex plane of the perturbed matrix, when the original matrix \hat{M} is subjected to all possible complex perturbations of a magnitude of the order of ε . Mathematically we have:

$$\sigma_\varepsilon(\hat{M}) \equiv \bigcup_{m=1, \|\hat{E}_m\| < \varepsilon}^{N_r} \sigma(\hat{M} + \hat{E}_m), \quad (27)$$

where N_r is the number of realizations of the full non-Hermitian random matrix \hat{E} , and the parameter ε characterizes the strength of the random perturbations. The union of all these spectra of the N_r perturbed matrices is the pseudospectrum. An alternative definition in terms of the matrix resolvent of \hat{M} is the following:

$$\sigma_\varepsilon(\hat{M}) \equiv \{z \in \mathcal{C} : \|(z\hat{I} - \hat{M})^{-1}\| > \varepsilon^{-1}\}, \quad (28)$$

where \hat{I} is the identity matrix and the $R(z) \equiv (z\hat{I} - \hat{M})^{-1}$ is the resolvent of the matrix \hat{M} , and z is any complex number $z = x + iy \in \mathcal{C}$ (not to be confused with the z -propagation distance symbol). Instead of only looking at the singularities of the matrix resolvent (which correspond to the eigenvalues

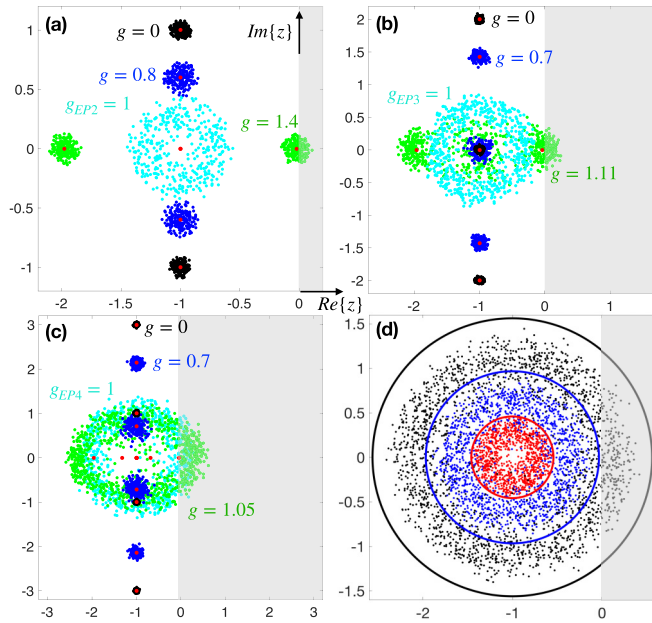


FIG. 4. (a), (b), (c) Pseudospectra $\sigma_{0,1}(\hat{M})$ of the three matrices $\hat{M}_2, \hat{M}_3, \hat{M}_4$, respectively, for different values of the parameter g in the complex plane. In all three figures the red dots correspond to the eigenvalues of the matrices. Different pseudospectra correspond to different colors and values of g and they have been calculated based on the first definition of the spectra of the perturbed matrices. (d) Pseudospectra on the complex plane of the three matrices exactly at the HEPs ($g = 1, l = 1$). In particular with red, blue, black clouds are shown the $\sigma_{0,1}(\hat{M}_2), \sigma_{0,1}(\hat{M}_3), \sigma_{0,1}(\hat{M}_4)$ pseudospectra, respectively. The corresponding solid curves of the same color are the level curves for $\epsilon = 0.1$ based on the second definition (matrix resolvent level curves).

of \hat{M} , we are interested in the level curves of the matrix resolvent, which leads us to pseudospectrum. The third definition is based on singular values of the matrix $z\hat{I} - \hat{M}$, namely:

$$\sigma_\epsilon(\hat{M}) \equiv \{z \in \mathcal{C} : \min[s(z\hat{I} - \hat{M})] < \epsilon\}. \quad (29)$$

Practically speaking, the pseudospectrum $\sigma_\epsilon(\hat{M})$ is a pattern in the complex plane that shows how sensitive the eigenvalue spectrum $\sigma(\hat{M})$ is to random perturbations. Additionally, it provides valuable information regarding the transient growth dynamics [1]. For hermitian operators the spectrum and the pseudospectrum are almost identical. But for non-Hermitian operators the two patterns can differ significantly, depending on the degree of the nonorthogonality of the corresponding eigenmodes.

Before everything else it is important to calculate the pseudospectra for the three matrices of interest, namely $\sigma_{0,1}(\hat{M}_2), \sigma_{0,1}(\hat{M}_3), \sigma_{0,1}(\hat{M}_4)$, based on the first definition. Our results are illustrated in Fig. 4. More specifically, the trajectories of the pseudospectra on the complex plane for different values of g (different colored clouds correspond to the value of g with the corresponding color), are shown for the three matrices in Figs. 4(a)–4(c), respectively. The red dots that represent the eigenvalues are also shown for reference. In Fig. 4(d) we present the 0.1 pseudospectra (red for \hat{M}_2 , blue for \hat{M}_3 , and black for \hat{M}_4) exactly at the EP2, EP3, EP4 exceptional points for $g = 1$. The corresponding solid curves (red, blue, black)

are the 0.1 pseudospectra based on the second definition of pseudospectra on matrix resolvent. The extend of the pseudospectra clouds show their sensitivity against perturbations and as is expected is maximum at EPN's [Fig. 4(d)] [57,59].

Since we are interested on power growth dynamics, a useful related quantity is the pseudospectral abscissa $\alpha_\epsilon(\hat{M})$ of \hat{M} that is defined as [1]:

$$\alpha_\epsilon(\hat{M}) \equiv \max\{\text{Re}(z) : z \in \sigma_\epsilon(\hat{M})\}, \quad (30)$$

which is the maximum real part of any point belonging on the ϵ pseudospectrum. Now the extend of the pseudospectrum cloud into the right half of the complex plane (gray-shaded area in Fig. 4) relative to ϵ is a criterion for the existence of transient growth. The geometrical characteristics of the pseudospectrum cloud are directly related to the power growth dynamics of the governing coupled mode equations. As such, we are interested to find order of magnitude estimates for the G_{\max}^{\max} in order to characterize our systems. In particular, an upper and lower bound of G_{\max}^{\max} can be estimated by applying the Kreiss matrix theorem of functional analysis of non-normal operators [1–4]. Let us first define a related constant that is directly related to the pseudospectral abscissa $\alpha_\epsilon(\hat{M})$. The Kreiss constant \mathcal{K} of the matrix \hat{M} is defined as:

$$\mathcal{K}(\hat{M}) \equiv \sup_{\epsilon > 0} \frac{\alpha_\epsilon(\hat{M})}{\epsilon} \quad (31)$$

or equivalently based on the matrix resolvent, with respect to the right half of the complex plane:

$$\mathcal{K}(\hat{M}) \equiv \sup_{\text{Re}z > 0} \{\text{Re}z | |(z\hat{I} - \hat{M})^{-1}|\}. \quad (32)$$

Now the Kreiss matrix theorem for any complex matrix $N \times N$ can be stated as [1,3,4]:

$$\mathcal{K}(\hat{M}) \leq \sup_{z \geq 0} \|e^{z\hat{M}}\| \leq eN\mathcal{K}(\hat{M}), \quad (33)$$

where e is the Euler's number. Such a theorem provides a lower and an upper bound on the value of G_{\max}^{\max} .

Let us now apply the Kreiss matrix theorem to our problem and estimate mG_{\max}^{\max} . First of all, we note that the special case $\mathcal{K}(\hat{M}) = 1$, implies that we have no transient growth ($G_{\max}^{\max} = 1$) and similar discussion about the mathematical criteria for the existence of transient growth can be found in the context of the Hille-Yoshida theorem [73,74]. For example, when $g = g_{HEP} = 1$ [see Fig. 4(d)] one can examine when the extreme sensitivity around an EPN is enough to contribute to the transient growth for any value of N . For $N = 2, 3, 4$ one can calculate the corresponding pseudospectral abscissa and show that transient growth is impossible for $N = 2$, but exists for $N = 3$ and $N = 4$.

The second case of interest is when $g \approx g_c$, and is going to be systematically examined in what follows. The pseudospectra based on the third definition (singular values) are calculated in Fig. 5 for the maximum value of g that corresponds to transient growth, namely, when $g \approx g_c$. In particular, the pseudospectra $\sigma_\epsilon(\hat{M})$ of the three matrices $\hat{M}_2, \hat{M}_3, \hat{M}_4$, respectively, are shown in Figs. 5(a)–5(c). The white solid level curves correspond to different values of ϵ . The magnified areas of the complex plane [marked with orange dashed square in Figs. 5(a)–5(c)] presented in Figs. 5(d)–5(f) help

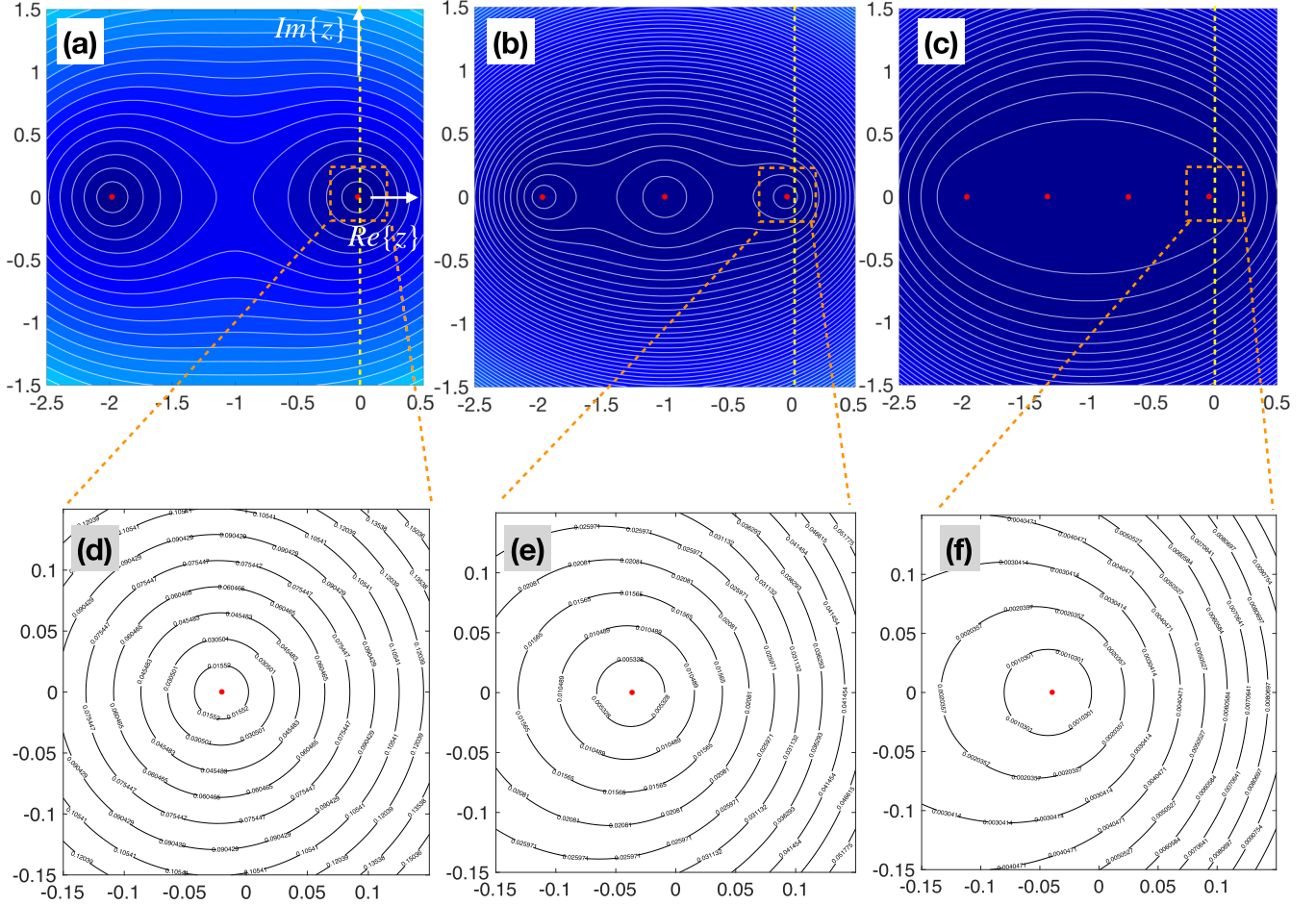


FIG. 5. (a), (b), (c) Pseudospectra $\sigma_\varepsilon(\hat{M})$ of the three matrices $\hat{M}_2, \hat{M}_3, \hat{M}_4$, respectively, for different values of ε , calculated based on the third definition of pseudospectra. The level curves (white solid lines) correspond to different values of ε . The values of the parameter g here are 1.4, 1.11, 1.05, respectively. In all three figures the red dots correspond to the eigenvalues of the matrices and the vertical dashed-yellow line the imaginary axis of the complex plane. (d), (e), (f) Magnification of the (a), (b), (c) figures around the dashed-orange square area of the complex plane. All figures here are plotted in the complex plane.

us to numerically evaluate the pseudospectral abscissa. The Kreiss constant based on both definitions for our problem is: $\mathcal{K}(\hat{M}_2(g = 1.4)) \approx 1.249$ (1.209), $\mathcal{K}(\hat{M}_3(g = 1.11)) \approx 3.411$ (3.55), $\mathcal{K}(\hat{M}_4(g = 1.05)) \approx 17.88$ (17.82), where the second number in the parentheses is the result based on the first definition. The agreement between the two definitions is very good and is limited only by the grid resolution. Based on the Kreiss matrix theorem we have the bounds: $1.249 \leq \sqrt{G_{\max}^{\max}} \leq 6.79$, $3.411 \leq \sqrt{G_{\max}^{\max}} \leq 27.82$, $17.88 \leq \sqrt{G_{\max}^{\max}} \leq 194.5$, where the exact values of G_{\max}^{\max} are 1.358, 4.433, and 26.238, respectively (with the first two values to be close to mG_{\max}^{\max}). The agreement between the exact (singular value decomposition) and the approximate approach (pseudospectrum) is pretty good and thus the Kreiss constant can be used to estimate the order of magnitude of G_{\max}^{\max} , and of mG_{\max}^{\max} . In a similar way the maximal growth can be estimated for different values of the parameter g .

VII. EFFECT OF LOSS ON TRANSIENT GROWTH

In this last section we are going to systematically examine the effect of the overall loss on the values of the maximum

transient growth. So far we have considered $l = 1$ and we are interested to examine what happens to mG_{\max}^{\max} for different values of the loss parameter l . Before we continue, let us introduce the most general expression of a matrix \hat{M}_N that exhibits a HEP of order N , which is given by the following tridiagonal $N \times N$ matrix [71]:

$$\hat{M}_N = i \begin{bmatrix} ig_0 + il & \kappa_0 & 0 \dots & 0 \\ \kappa_0 & ig_1 + il & \kappa_1 \dots & 0 \\ \dots & \dots & \dots & \dots \\ 0 \dots & \kappa_{N-1} & ig_{N-2} + il & \kappa_{N-2} \\ 0 \dots & 0 & \kappa_{N-2} & ig_{N-1} + il \end{bmatrix}, \quad (34)$$

where $g_{\tilde{n}} \equiv g(2\tilde{n} - N + 1)$, the coupling coefficients are $\kappa_{\tilde{n}} \equiv \kappa \sqrt{(\tilde{n} + 1)(N - \tilde{n} - 1)}$, and the integer index takes values $\tilde{n} = 0, 1, 2, \dots, N - 1$. As before we assume $\kappa = 1$ and we know that the EPN occurs for $g_{HEP} = 1$ at the $(-l, 0)$ point of the complex plane.

Regarding now the effect of the overall loss parameter we have calculated the maximal growth based on the singular value decomposition method. Our results are illustrated in Fig. 6, where we have plotted the mG_{\max}^{\max} versus l for different

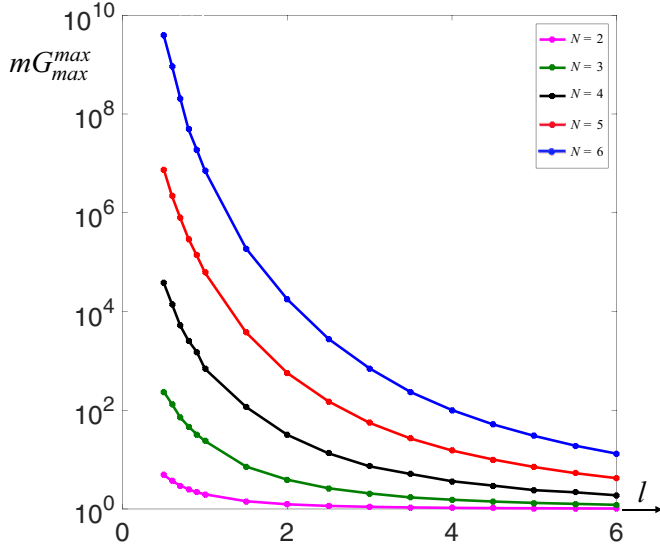


FIG. 6. Dependence of the mG_{\max}^{\max} on the loss parameter l , for different order of the EPN. In particular, the maximal value of the transient growth over all values of g for various values of the overall loss parameter l , is plotted in logarithmic scale for $N = 2, 3, 4, 5, 6$ with magenta-green-black-red-blue lines, for each matrix that exhibit an EPN, respectively.

values of $N = 2, 3, 4, 5, 6$. In all cases, the limit of $l \rightarrow 0$ corresponds to very high values of transient growth. This is expected since for the case $l = 0$ we have the analytical power-law expression $G_{\max}^{\max} = \left(\frac{1+g}{1-g}\right)^{N-1}$ [71]. On the other hand, as we increase the loss parameter, the values of G_{\max}^{\max} decrease but still transient growth is possible. In fact, it is possible to achieve amplification even if the material loss is much higher than the material gain.

Such an effect strongly depends on the order of the EPN. For example when $N = 6$ and $l = 6$, the maximum material loss is the last diagonal element of the \hat{M}_N matrix namely $\hat{M}_N(N, N) = -g_{N-1} - l = -g(N-1) - l < 0$ whereas the maximum material gain is the first one $\hat{M}_N(1, 1) = -g_0 - l = g(N-1) - l$. The maximal transient growth $mG_{\max}^{\max}(g = 1.56) \approx 13$ even though $\frac{|\hat{M}_6(6,6)|}{\hat{M}_6(1,1)} \approx 7.6$, whereas the corresponding growth for $N = 2$ and $l = 6$ is almost one. This physically means that by increasing the order of the EPN we can have significant transient amplification of the optimal initial conditions in a physical waveguide system, where material

loss largely dominates over material gain. This is particularly important for various photonic applications, where usually the access to gain materials is difficult and expensive, whereas the materials used are inherently lossy (active plasmonics, for example).

VIII. CONCLUSIONS

In summary, we have presented a general methodology for studying the physics of transient growth [73–76] in any finite-dimensional dynamical system that involves a non-normal evolution matrix with dissipative HEP. The physical context of our results is that of non-Hermitian photonics, where material gain (laser systems) and loss are physically accessible and relevant. The particular non-Hermitian system of interest is that of coupled optical waveguides that contain gain and loss and exhibit higher-order exceptional points (dissipative EPN's). The whole complex spectrum of the coupled structure is shifted into the left-half part of the complex plane, by applying a global gauge transformation. Physically this is equivalent to adding a uniform loss to all channels. We identify three distinct regimes depending on the value of the gain-loss amplitude g : dissipation, transient growth, and amplification. Due to the fact that the eigenstates are nonorthogonal, it is physically possible to have power transient amplification even though all eigenvalues correspond to decay. This means that in order to understand the underlying physics of transient growth we cannot rely on our notion of eigenvalues, but we have to employ different approaches. More specifically, we follow three different but related paths: norm of the exponential matrix (exact), singular value decomposition (exact), and pseudospectra (geometric-approximate). We systematically study the maximal transient growth for any value of the involved parameters and determine the corresponding optimal initial conditions. Based on the increased non-normality degree that depends on the order of the EPN, we can achieve significant transient amplification in structures that are characterized by high material loss and low material gain. This is particularly important for various integrated photonics applications that involve inherently lossy materials where power amplification is crucial.

ACKNOWLEDGMENT

The author acknowledges helpful and constructive discussions with Ramy El-Ganainy and Ziad Musslimani.

- [1] L. N. Trefethen and M. Embree, *Spectra and Pseudospectra*, (Princeton University Press, Princeton, 2005).
- [2] L. N. Trefethen, A. E. Trefethen, S. C. Reddy, and T. A. Driscoll, *Science* **261**, 578 (1993).
- [3] L. N. Trefethen, *SIAM Rev.* **39**, 383 (1997).
- [4] L. N. Trefethen, *Acta Num.* **8**, 247 (1999).
- [5] G. Hennequin, T. P. Vogels, and W. Gerstner, *Phys. Rev. E* **86**, 011909 (2012).
- [6] S. Nicoletti, N. Zagli, D. Fanelli, R. Livi, T. Carletti, and G. Innocenti, *Phys. Rev. E* **98**, 032214 (2018).
- [7] G. Baggio *et al.*, *Sci. Adv.* **6**, eaba2282 (2020).
- [8] T. Gebhardt and S. Grossmann, *Phys. Rev. E* **50**, 3705 (1994).
- [9] J. L. Jaramillo, R. P. Macedo, and L. A. Sheikh, *Phys. Rev. X* **11**, 031003 (2021).
- [10] K. Petermann, *IEEE J. Quantum Electron.* **15**, 566 (1979).
- [11] M. V. Berry, *J. Mod. Opt.* **50**, 63 (2003).
- [12] Yuh-Jen Cheng, C. G. Fanning, and A. E. Siegman, *Phys. Rev. Lett.* **77**, 627 (1996).
- [13] A. E. Siegman, *Phys. Rev. A* **39**, 1253 (1989).
- [14] A. E. Siegman, *J. Opt. Soc. Am. A* **20**, 1617 (2003).

- [15] A. E. Siegman, *Appl. Phys. B* **60**, 247 (1995)
- [16] A. Kostenbauder, Y. Sun, and A. E. Siegman, *J. Opt. Soc. Am. A* **14**, 1780 (1997).
- [17] D. N. Christodoulides, F. Lederer, and Y. Silberberg, *Nature (London)* **424**, 817 (2003).
- [18] C. M. Bender and S. Boettcher, *Phys. Rev. Lett.* **80**, 5243 (1998).
- [19] C. M. Bender, D. C. Brody, and H. F. Jones, *Phys. Rev. Lett.* **89**, 270401 (2002).
- [20] C. M. Bender, *Rep. Prog. Phys.* **70**, 947 (2007).
- [21] R. El-Ganainy, K. G. Makris, D. N. Christodoulides, and Z. H. Musslimani, *Opt. Lett.* **32**, 2632 (2007).
- [22] K. G. Makris, R. El-Ganainy, D. N. Christodoulides, and Z. H. Musslimani, *Phys. Rev. Lett.* **100**, 103904 (2008).
- [23] Z. H. Musslimani, K. G. Makris, R. El-Ganainy, and D. N. Christodoulides, *Phys. Rev. Lett.* **100**, 030402 (2008).
- [24] K. G. Makris, R. El-Ganainy, D. N. Christodoulides, and Z. H. Musslimani, *Phys. Rev. A* **81**, 063807 (2010).
- [25] A. Guo, G. J. Salamo, D. Duchesne, R. Morandotti, M. Volatier-Ravat, V. Aimez, G. A. Siviloglou, and D. N. Christodoulides, *Phys. Rev. Lett.* **103**, 093902 (2009).
- [26] C. E. Rüter, K. G. Makris, R. El-Ganainy, D. N. Christodoulides, M. Segev, and D. Kip, *Nat. Phys.* **6**, 192 (2010).
- [27] O. Bendix, R. Fleischmann, T. Kottos, and B. Shapiro, *Phys. Rev. Lett.* **103**, 030402 (2009).
- [28] H. Ramezani, T. Kottos, R. El-Ganainy, and D. N. Christodoulides, *Phys. Rev. A* **82**, 043803 (2010).
- [29] M. C. Zheng, D. N. Christodoulides, R. Fleischmann, and T. Kottos, *Phys. Rev. A* **82**, 010103(R) (2010).
- [30] Y. D. Chong, L. Ge, and A. D. Stone, *Phys. Rev. Lett.* **106**, 093902 (2011).
- [31] L. Ge, Y. D. Chong, and A. D. Stone, *Phys. Rev. A* **85**, 023802 (2012).
- [32] J. D. H. Rivero, M. Pan, K. G. Makris, L. Feng, and L. Ge, *Phys. Rev. Lett.* **126**, 163901 (2021).
- [33] L. Ge and A. D. Stone, *Phys. Rev. X* **4**, 031011 (2014).
- [34] N. Lazarides and G. P. Tsironis, *Phys. Rev. Lett.* **110**, 053901 (2013).
- [35] G. Castaldi, S. Savoia, V. Galdi, A. Alu, and N. Engheta, *Phys. Rev. Lett.* **110**, 173901 (2013).
- [36] J. Ctyrosky, V. Kuzmiak, and S. Eyderman, *Opt. Express* **18**, 21585 (2010).
- [37] H. Benisty *et al.*, *Opt. Express* **19**, 18004 (2011).
- [38] A. Lupu, H. Benisty, and A. Derigon, *Opt. Express* **21**, 21651 (2013).
- [39] A. Regensburger, C. Bersch, M.-A. Miri, G. Onishchukov, D. N. Christodoulides, and U. Peschel, *Nature (London)* **488**, 167 (2012).
- [40] L. Feng, Y.-L. Xu, W. S. Fegadolli, M.-H. Lu, J. E. B. Oliveira, V. R. Almeida, Y.-F. Chen, and A. Scherer, *Nat. Mater.* **12**, 108 (2013).
- [41] B. Peng, S. K. Özdemir, F. Lei, F. Monifi, M. Gianfreda, G. L. Long, S. Fan, F. Nori, C. M. Bender, and L. Yang, *Nat. Phys.* **10**, 394 (2014).
- [42] L. Feng, Z. Jing Wong, R.-M. Ma, Y. Wang, and X. Zhang, *Science* **346**, 972 (2014).
- [43] H. Hodaie, M.-A. Miri, M. Heinrich, D. N. Christodoulides, and M. Khajavikhan, *Science* **346**, 975 (2014).
- [44] B. Peng, S. K. Özdemir, S. Rotter, H. Yilmaz, M. Liertzer, F. Monifi, C. M. Bender, F. Nori, and L. Yang, *Science* **346**, 328 (2014).
- [45] S. Assaworarrarit, X. Yu, and S. Fan, *Nature (London)* **546**, 387 (2017).
- [46] J. Zhang, B. Peng, S. K. Özdemir, K. Pichler, D. O. Krimer, G. Zhao, F. Nori, Y. Liu, S. Rotter, and L. Yang, *Nat. Photon.* **12**, 479 (2018).
- [47] S. Xia, D. Kaltsas, D. Song, I. Komis, J. Xu, A. Szameit, H. Buljan, K. G. Makris, and Z. Chen, *Science* **372**, 72 (2021).
- [48] I. Rotter, *Phys. Rev. E* **67**, 026204 (2003).
- [49] M. V. Berry, *Czech. J. Phys.* **54**, 1039 (2004).
- [50] W. D. Heiss, *J. Phys. A: Math. Gen.* **37**, 2455 (2004).
- [51] M. H. Teimourpour, R. El-Ganainy, A. Eisfeld, A. Szameit, and D. N. Christodoulides, *Phys. Rev. A* **90**, 053817 (2014).
- [52] W. D. Heiss, *J. Phys. A* **45**, 444016 (2012).
- [53] J. Wiersig, S.-W. Kim, and M. Hentschel, *Phys. Rev. A* **78**, 053809 (2008).
- [54] S.-B. Lee, J. Yang, S. Moon, S.-Y. Lee, J.-B. Shim, S. W. Kim, J.-H. Lee, and K. An, *Phys. Rev. Lett.* **103**, 134101 (2009).
- [55] E. M. Graefe, U. Gunther, H. J. Korsch, and A. E. Niederle, *J. Phys. A* **41**, 255206 (2008).
- [56] D. Gilles and E. M. Graefe, *J. Phys. A* **45**, 025303 (2012).
- [57] J. Wiersig, *Phys. Rev. Lett.* **112**, 203901 (2014).
- [58] J. Wiersig, *Phys. Rev. A* **93**, 033809 (2016).
- [59] H. Hodaie, A. U. Hassan, S. Wittek, H. Garcia-Gracia, R. El-Ganainy, D. N. Christodoulides, and M. Khajavikhan, *Nature (London)* **548**, 187 (2017).
- [60] T. Kottos, *Nat. Phys.* **6**, 166 (2010).
- [61] V. V. Konotop, J. Yang, and D. A. Zezyulin, *Rev. Mod. Phys.* **88**, 035002 (2016).
- [62] L. Feng, R. El-Ganainy, and L. Ge, *Nat. Photon.* **11**, 752 (2017).
- [63] D. F. Pile and D. N. Christodoulides, *Nat. Photon.* **11**, 742 (2017).
- [64] G. Gbur and K. G. Makris, *Photon. Res.* **6**, PTS1 (2018).
- [65] R. El-Ganainy, K. G. Makris, M. Khajavikhan, Z. H. Musslimani, S. Rotter, and D. N. Christodoulides, *Nat. Phys.* **14**, 11 (2018).
- [66] S. K. Özdemir, S. Rotter, F. Nori, and L. Yang, *Nat. Mater.* **18**, 783 (2019).
- [67] M. A. Miri and A. Alu, *Science* **363**, eaar7709 (2019).
- [68] S. Longhi and P. Laporta, *Phys. Rev. E* **61**, R989 (2000).
- [69] F. Papoff, G. D'Alessandro, and G. L. Oppo, *Phys. Rev. Lett.* **100**, 123905 (2008).
- [70] K. G. Makris, L. Ge, and H. E. Türeci, *Phys. Rev. X* **4**, 041044 (2014).
- [71] Q. Zhong, D. N. Christodoulides, M. Khajavikhan, K. G. Makris, and R. El-Ganainy, *Phys. Rev. A* **97**, 020105(R) (2018).
- [72] J. Wiersig, *Phys. Rev. Research* **1**, 033182 (2019).
- [73] S. C. Reddy, P. J. Schmid, and D. S. Henningson, *SIAM J. Appl. Math.* **53**, 15 (1993).
- [74] S. C. Reddy and D. S. Henningson, *J. Fluid Mech.* **252**, 209 (1993).
- [75] J. S. Baggett, T. A. Driscoll, and L. N. Trefethen, *Phys. Fluids* **7**, 833 (1995).
- [76] P. J. Schmid, *Phys. Plasmas* **7**, 1788 (2000).